Revealing metabolic mechanisms of interaction in the anaerobic digestion microbiome by flux balance analysis

Basile, Arianna; Campanaro, Stefano; Kovalovszki, Adam; Zampieri, Guido; Rossi, Alessandro; Angelidaki, Irini; Valle, Giorgio; Treu, Laura

Published in:
Metabolic Engineering

Link to article, DOI:
10.1016/j.ymben.2020.08.013

Publication date:
2020

Document Version
Peer reviewed version

Revealing metabolic mechanisms of interaction in the anaerobic digestion microbiome by flux balance analysis

Arianna Basile, Stefano Campanaro*, Adam Kovalovszki, Guido Zampieri, Alessandro Rossi, Irini Angelidaki, Giorgio Valle§, Laura Treu§

* corresponding author: stefano.campanaro@unipd.it

§ equal contribution

Abstract

Anaerobic digestion is a key biological process for renewable energy, yet the mechanistic knowledge on its hidden microbial dynamics is still limited. The present work charted the interaction network in the anaerobic digestion microbiome via the full characterisation of pairwise interactions and the associated metabolite exchanges. To this goal, a novel collection of 836 genome-scale metabolic models was built to represent the functional capabilities of bacteria and archaea species derived from genome-centric metagenomics. Dominant microbes were shown to prefer mutualistic, parasitic and commensalistic interactions over neutralism, amensalism and competition, and are more likely to behave as metabolite importers and profiteers of the coexistence. Additionally, external hydrogen injection positively influences microbiome dynamics by promoting commensalism over amensalism. Finally, exchanges of glucogenic amino acids were shown to overcome auxotrophies caused by an incomplete tricarboxylic acid cycle. Our novel strategy predicted the most favourable growth conditions for the microbes, overall suggesting strategies to increasing the biogas production efficiency. In principle, this approach could also be applied to microbial populations of biomedical importance, such as the gut microbiome, to allow a broad inspection of the microbial interplays.

Keywords

Anaerobic digestion/flux balance analysis/genome-scale metabolic models/microbial interactions/renewable energy

1. Introduction

Microorganisms play an important role in all fields of biological relevance, ranging from human health (Clemente et al., 2012) to biotechnology (Lebuhn et al., 2015). In particular, diverse microbiomes may have various responsibilities, from causing diseases to influencing applied processes (e.g. biogas production) (Zhu et al., 2020) or the synthesis of polymeric substances (Chow et al., 2008). Microbial networks, however, are still poorly understood due to difficulties in isolating most of the microbial species and to the heterogeneous nature of their interactions (Muller et al., 2018). While the inspection of a core microbiome might reveal which species are the key players for a specific process (Faith, 2015), the role of rare members still remains to be clarified (Jousset et al., 2017). Microbial cooperation is extremely important for environmental niche colonization and completing complex activities (Stolyar et al., 2007), which single species could not perform independently (Hay et al., 2004). This is the case in anaerobic digestion (AD), which is a biotechnological process that produces a potent renewable energy carrier called biogas (Yentekakis and Goula, 2017). During biogas production, when acetoclastic methanogenic archaea are inhibited, a pivotal role is played by hydrogenotrophic methanogenic archaea and syntrophic acetate oxidizing bacteria (Mosbæk et al., 2016) (SAOB). An example is the mutualism between the hydrogen-utilizing methanogen *Methanoculleus bourgensis* and the SAOB *Syntrophaceticus schinkii*, *[Clostridium] ultunense*, and *Tepidanaerobacter acetatoxydans* (Westerholm et al., 2019). SAOB oxidise acetate to formate or to H_2 and carbon dioxide (CO_2). The bacteria rely on archaeal activity, because acetate oxidation rapidly becomes endergonic when H_2 accumulates (Stams

and Plugge, 2009). Indeed, subsequently H_2-utilizing methanogens convert these substrates to methane (CH_4) (Treu et al., 2018).

Although direct microbial cultivation and phenotyping experiments are essential to investigate metabolite exchanges and species interplays, this is not always possible. In fact, several microbes responsible for important biotechnological processes cannot be isolated and investigated using classical microbiological approaches because their specific growth demands are unknown, or because they cannot grow without the simultaneous existence of synergistic partners (Shlomi et al., 2007). In order to access the vast fraction of uncultivable microbes, genome centric metagenomics has given new possibilities to the scientific community (Parks et al., 2017).The extraction of genomes from complex assemblies allows the inference of metabolic pathways present in Metagenome Assembled Genomes (MAGs) (Nayfach et al., 2019), using the Kyoto Encyclopedia of Genes and Genomes database (KEGG) (Kanehisa et al., 2016) and/or EcoCyc (Keseler et al., 2017). Unfortunately, the use of gene annotation alone cannot fully describe the role of each microbial species in the global metabolic network mainly because many of the functions and reactions are still unknown (Zacher et al., 2014). Thus, a novel approach is needed for deciphering functional roles, microbial interactions and the exchange of molecules. Flux balance analysis (FBA) of *in silico* metabolic networks has recently emerged as one of the most effective methods to unveil microbial interplays (Magnúsdóttir et al., 2017). In fact, such metabolic models account for known intracellular processes (Budinich et al., 2017), as well as for metabolite uptake and secretion. This approach offers a reliable representation of the cross feeding occurring between community members (Khandelwal et al., 2013), and is able to predict how species gather in large consortia (Machado et al., 2020). However, previous studies relied on microbial consortia derived by 16S-based metagenomes to recover either the closest genomes or models publicly available in database. This assumption may limit the accuracy of the analysis as the correspondence between 16S-derived information and public data may be imprecise. Furthermore, microbial species can activate different pathways according

to the growth medium and the relationship among different members of the same consortia. Metatranscriptomic results can be integrated to constrain the metabolic models and confirm previously flux balance analysis results. The ability to predict the structure and functioning of complex microbiomes is crucial for the study of organic matter degradation (Boon et al., 2014). The AD community is able to produce methane through a biologically mediated process, which is one of the oldest bioactivities on Earth (Sorokin et al., 2017). Anaerobic organic matter degradation naturally occurs in many ecological niches including, for example, the digestive tract of animals and anaerobic sediments (Liebetrau et al., 2019). Moreover, the biotechnological relevance is clear, as it can be exploited for biogas production. From an anthropocentric point of view, the AD microbiome organization can be visualized as a funnel (Campanaro et al., 2020) with methane as the final product. The funnel concept represents the progressive functional specialization, where the microbial players can be classified into four groups: hydrolytic, acidogenic and acetogenic bacteria, and methanogenic archaea (Campanaro et al., 2016). In the last few years, biotechnological applications in renewable energy and CO_2 sequestration fields have been under active development due to the increasing environmental awareness, which is leading to a lower fossil fuel dependency and to a more intelligent management of natural resources (Hall and Scrase, 1998). During biogas production, the reactor efficiency can be increased through an accurate monitoring of process parameters, including temperature, mixing, reactor characteristics, feedstock composition (Angelidaki et al., 2018). All these factors can have a direct effect on the microbial community (Zhu et al., 2019). However, despite the microbiome's pivotal role in organic matter conversion into methane, there is still a lack of knowledge regarding the microbial influence on the process (Koch et al., 2019).

In order to unravel the microbial network and to clarify how process parameters can affect the microbiome structure, a FBA-based approach is proposed to explore metabolic exchanges in the AD community. Specifically, the objectives of the study were: a) to apply and develop a flux balance-based method for analysing coexistence

dynamics in microbial consortia; b) to set-up a pipeline for the inspection of both microbial pairwise interactions and metabolites exchanges considering also the implementation of metatranscriptomic data to constrain the solution space; c) to investigate the interdependencies among multiple species, d) to define a comprehensive metabolic model of the AD microbiome. Additionally, bioinformatics approaches were used to understand how cross-feeding varies according to the different experimental conditions and simultaneous metabolite exchange among multiple species were investigated by analysing the flux network (Chaffron et al., 2010).

2. Results

The microbial species selected to be included as case study account for both archaea and bacteria and constitute the biggest known database of AD microbiome derived from metagenomic data (Campanaro et al., 2020). Of the reconstructed MAGs, only 836 have been considered for genome-scale metabolic model (GSMMs) reconstruction, which were identified as “high quality” regarding their genome completeness and contamination according to MIMAG guidelines (Bowers et al., 2017). These MAGs were taxonomically associated to 30 phyla involved in the AD process (Supplementary Table I) and represented the initial step of the investigation into interphylum and inter-kingdom interactions occurring in the anaerobic microbiome. The large-scale assessment of microbial relationships was performed in two stages, considering a feedstock rich in sugar and proteins in the former and the influence of external H_2 injection in the latter (Treu et al., 2019). Subsequently, four different populations of the microbiome were used to analyse the occurring metabolic mechanisms and to determine the microbial interactivity. In this case, only the MAGs having a relative abundance higher than 0.001% were considered, based on the results of a previous experiment (Fontana et al., 2018) and using a feedstock rich in sugar and proteins. The first two populations were methanogenic, responsible for

methane production before and after H_2 injection, while the other two were acidogenic and governed the production of acetate and other volatile fatty acids (VFA).

Upon reconstruction, each model underwent a battery of quality control tests to verify biological and formal soundness. All models have full correspondence between reactions and genes, have demand reactions with fluxes in backward direction and pass the single gene deletion tests. The “leak tests” reports a score higher than 0.99 in all GSMMs (both with and without demand reactions) (Supplementary Table II). Moreover, we benchmarked our models against those from a previous large-scale collection of human gut microbiome GSMMs based on the MEMOTE tool (Lieven et al., 2020). This comparison highlighted a few systematic differences between the GSMM collections, probably due to the use of different model reconstruction software, some of which were already observed by Lieven and colleagues (Lieven et al., 2020) (Appendix and Figshare 10.6084/m9.figshare.12582746.v2). In particular, MEMOTE results revealed that AGORA models have a more complete GPR annotation and a lower number of mass-unbalanced reactions. However, models generated with CarveMe have a lower number of blocked reactions and so-called “orphan metabolites”.

In total, 4132 unique metabolic reactions, involving 1580 different compounds, were identified. Each GSMM included on average 1391±245 reactions, 1012±152 metabolites and 571±159 genes (Fig. 1A and Supplementary Table II). 112 metabolites (7%) (e.g. L-Tryptophan, L-Valine, L-Tyrosine, Glycine, L-Methionine) and many cofactors (e.g. FAD, FADH, NMN, $NADP^+$, $NADPH_2$) were predicted in all models and were identified as “microbiome metabolite core”, while 36 compounds were specific to individual models and were defined as “microbiome metabolite cloud”. The presence and completeness of pathways responsible for carbohydrate and lipid metabolism have been tested in the metabolic models by tracking the corresponding reactions. Regarding carbohydrate metabolism, *Actinomycetales* sp. GSMM1485, *Clostridiaceae* sp. GSMM0156, *Clostridiales* spp. GSMM0297, GSMM0760, GSMM1021, *Firmicutes* spp. GSMM0866, GSMM0213, *Tepidanaerobacter*

syntrophicus GSMM0017 were shown to have the complete anabolic and catabolic pathways. Regarding lipids metabolism, “beta-Oxidation, acyl-CoA synthesis” and “Phosphatidylethanolamine (PE) biosynthesis, PA => PS => PE” are complete in 18 GSMMs obtained from species belonging to the phylum Proteobacteria (Supplementary Table II).

When considering the taxonomic assignment of MAGs at phylum level, some phyla had an average smaller number of genes, metabolites and reactions (Fig. 1A), with the microbial species assigned to the *Synergistetes* phylum showing the lowest number of genes recorded. On the other hand, *Proteobacteria* had the highest number of genes, followed by *Acidobacteria*, *Actinobacteria* and *Armatimonadetes*. This result shows consistency with microbes belonging to *Proteobacteria* being considered “generalist”, as they can simultaneously perform multiple steps in the AD process, such as fatty acid degradation, butanoate metabolism, propionate metabolism, sulphate reduction and denitrification. This is in agreement with a previously reported study (Kitano, 2007).

A complete description of the metabolic potential present in the microbiome and the identification of new biochemical and physiological traits (both expected and non-intuitive) were accomplished by evaluating the 4132 biochemical reactions represented in the models. Only 33 “core reactions” were ubiquitously identified in all the microbes, which could be classified in three main categories: “transporters of simple molecules”, “kinases” and “transferases”. Moreover, methane biosynthesis was found in all the 29 archaeal species belonging to the *Euryarchaeota* phylum. A verification performed on the models by taking into account a set of 14 reactions revealed that *Methanosarcina* spp. (e.g. GSMM0042, GSMM0744, GSMM0883) can perform all the three methanogenic processes (acetoclastic, hydrogenotrophic and methylotrophic) as expected, while *Euryarchaeota* sp. GSMM0884, *Thermoplasmatales* Incertae Sedis sp. GSMM1074 and *Euryarchaeota* sp. GSMM0778 have a complete set of enzymes only for the methylotrophic methanogenesis (Supplementary Table II). Among the others, *Methanothermobacter*

spp. (e.g. GSMM0047 and GSMM0396) and *Methanoculleus* spp. (GSMM0046, GSMM0045) have been confirmed as hydrogenotrophs. *Methanothrix soehngenii* GSMM0064 and *Methanosaeta* sp. GSMM0125 have the complete acetoclastic pathway consistently with previous findings.

Conversely, 101 species-specific processes were defined as “shell reactions”. For instance, the model of *Clostridia* sp. GSMM1577 was the only one predicting the use of coproporphyrinogen as an intermediate for heme biosynthesis (Dailey et al., 2015). Similarly, only Candidatus *Riflebacteria* sp. GSMM0304 could import and metabolize L-gulonate and D-tagatose (Raspor and Goranovič, 2008). These monosaccharides are epimers and precursors of glucose-6-phosphate and precursors respectively of dihydroxyacetone phosphate and pyruvate (Heinken & Thiele, 2015). The unique characteristics of Candidatus *Riflebacteria* sp. GSMM0304 were related to CO utilization as a carbon source. In fact, this MAG was only present in a single experiment (Jing et al., 2017), suggesting its extreme specialization and possibly reflecting a low adaptability to survive in commonly utilised AD feedstocks. VFA, in particular acetate, propionate and butyrate are crucial intermediate compounds for the production of methane (Molina et al., 2009), as well as indicators of process stability (Jacobi et al., 2009) and agents for process diagnosis (Ahring et al., 1995). It is therefore extremely important to have a balance in the concentration of VFA, avoiding excessive accumulation of these intermediates in anaerobic reactors. The fundamental role of VFA in the AD system means that the possibility to estimate the intermediate compounds production and exchange in the AD microbiome is of great interest to tackle determinants of process instability (Liao et al., 2016). For this reason, the presence of genes involved in VFA production and utilization has been investigated in all the models (Fig. 1B). While some VFA, such as hexanoic, isovaleric and valeric acid were absent in the models, acetate was noticeably abundant, evidencing its association with the core microbial metabolism. According to the gene presence, the bacterial Wood–Ljungdahl pathway was identified as complete in nearly 40 species (Supplementary Table II). Regarding other VFA, propionate was reported

in 821 GSMMs, while butyrate in 693 (mainly in models of *Bacteroidetes* and *Synergistetes* species), which were respectively 98 and 82% of all GSMMs considered. In particular, propionate was involved in the biosynthesis of different key compounds belonging to the glycolytic pathway, including succinate, fumarate and oxaloacetate (Stryer, 1995). Assuming that the importance of different VFA in the cross-feeding process can be determined by the fraction of microbes which are able to exchange them, butyrate was probably one of the most relevant, since it was exchanged by 635 species. Propionate was exported by a lower number of microbes, suggesting a lower potential in cross-feedings. Among all VFA, isobutyrate was the rarest, being present in 61 models (or 7% of all GSMM) only. These results suggest that the cross-feeding of butyrate is common, consequently redundant in the microbiome, while the role of the few species involved in propionate exchange is crucial. Accordingly, an alteration in the abundance of the propionate producers might trigger a cascade effect, resulting in the loss of species utilizing this VFA to produce other important intermediate metabolic compounds, such as fumarate and oxaloacetate.

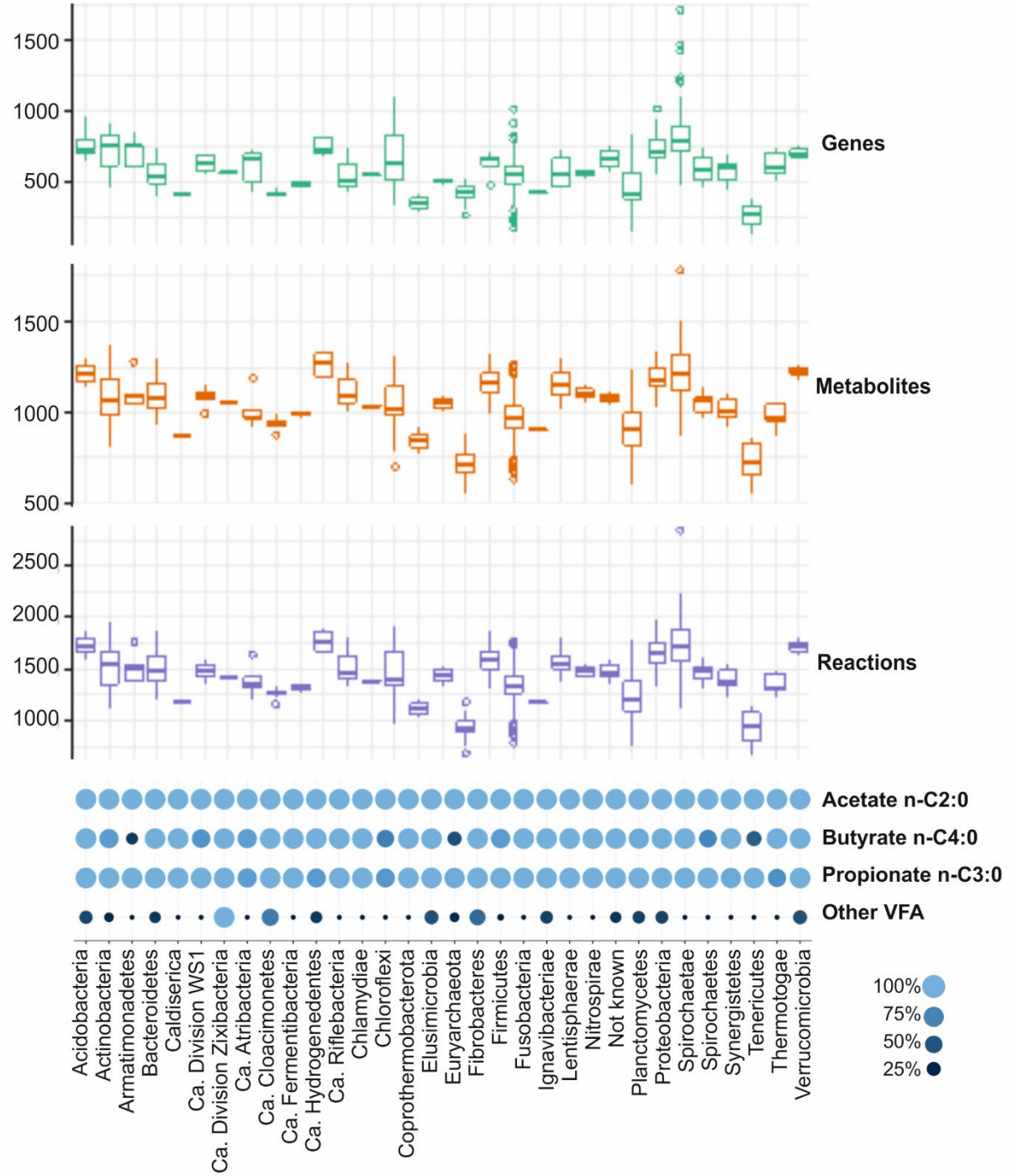

Fig. 1. General information of the metabolic models at phylum level.

Distribution of the number of genes, reactions and metabolites composing the reconstructed genome-scale metabolic models and presence of specific volatile fatty acids, divided by phylum. Whiskers show the minimum and maximum values. Values below “Q1 - 1.5 x IQR” and above “Q3 + 1.5 x IQR” are plotted as outliers (Q1: first quartile, Q3: third quartile, IQR: interquartile range). Colour and diameter of the circles depend on the fraction of microbes predicted to synthesize specific VFA.

2.1 Global landscape of pairwise interactions

The potential of 349,030 microbial couples being involved in positive or negative relationships was systematically investigated. In order to perform this investigation, PAirwise INteractivity analysis (PA.IN.), a computational framework for the prediction of interspecies behaviour was developed. Using the framework, different conditions (including hydrogen concentration) were investigated, obtaining in total 698,060 pairs. In the present work it was found impractical to perform simulations for interactions with order higher than two on 836 models due to computational and time effort, despite this type of analysis was previously applied (Machado et al., 2020).

Results revealed a variety of trade-offs within the microbe pairs depending on both the metabolic potential and the imposed environmental conditions. A comparative inspection of the relationships occurring between the 836 microbes, including those obtained for species belonging to the “rare biosphere”, was carried out to estimate the reciprocal potential impact of each species on the growth rate. This analysis was performed considering a diet designed *“ad hoc”* to simulate reactors’ feedstock rich in sugar and proteins (the exact medium composition is reported in subsection 4.2). Not all the GSMM groups could grow individually on this specific feedstock; however, all the models showed non-zero growth in at least one of the possible couples. The feedstock components description was obtained integrating data from the VMH database (Noronha et al., 2019) with measurements conducted on the “real” feeding substrate (Fontana et al., 2018). Additionally, results on the microbial community composition were obtained for the same feedstock, but for two different growth conditions, one specifically characterized by external H_2 injection. Hydrogen was supplemented to enhance the hydrogenotrophic methanogenesis and, consequently, to increase the methane content in the biogas, promoting the most important step of the process (Nugent et al., 2013). Due to the relevant role of H_2, both the shift in the functional activity of single microbes after injection and its influence on the microbial cross-talks were inspected.

Based on the modifications in the growth rate of a species occurring while engaging with another member of the microbiome, six different patterns were determined: parasitism (+/-), commensalism (+/0), neutralism (0/0), amensalism (-/0), competition (-/-) and mutualism (+/+) (where: + is positive, - is negative and 0 is no effect on each other between organisms) (Heinken and Thiele, 2015). When the coexistence negatively influences one of the two partners (growth rate decreases equal to or larger than 10%), the interplay is classified as negative, otherwise as positive. Neutralism is considered as a non-interaction, since the change in the growth rate derived from the microbial coexistence in the pair was included between -10% and +10%.

In the community, commensalism was identified in 33% of the pairs, indicating a general positive reciprocal influence occurring between microbes (Fig. 2A). This behaviour, frequently detected in biodegradation processes (Campanaro *et al*, 2020), is mediated by cross-feeding which is indeed favouring synergies. Furthermore, among negative interactions, competition is the rarest, found only in 1.6% of the pairs (Appendix, Table S1). Similar results were obtained, considering the microbial species analyzed before using the cooperative tradeoff algorithm (Diener et al., 2020). This analysis confirmed that positive interactions are more frequent than negative ones (Supplementary Table III). Interestingly, the interactivity pattern identified is markedly different than that identified in other microbial communities where negative cross-talks are dominant. In fact, Heinken and coll. (Heinken and Thiele, 2015) found that parasitism is the most frequent meta-communication in human gut microbiome, while mutualism is the rarest. Notably, vessels in AD are strictly anaerobic while the gut is mainly microaerophilic, indicating that anoxicity promotes positive interspecies communication. An additional analysis was performed considering different thresholds for defining interactions: ±1%, ±5%, ±15% and ±20%. The higher the threshold, the higher the number of neutralisms identified (Supplementary Table III). However, it can be concluded that the threshold was not influencing the detection of the specific behaviour characterizing the community. Despite setting the thresholds at 15% and 20% resulted in a higher number of neutral interplays in comparison to the

commensalisms, negative interactions remain always lower in number than the positive ones (even without considering neutralism as positive). Relevant trends underlying the general organization of the community were identified at phylum level. All phyla were involved in the six types of co-occurrences (except *Caldiserica* and *Chlamydia* which include very few species) (Supplementary table III); however, some preferential kinds of interaction were identified via a statistical analysis (p-value<e-16, chi-square test). In particular, some taxa are characterized by a specific pattern of interactivity (validated by Pearson's residuals): *Bacteroidetes,* for example, are frequently involved in neutralism and rarely in parasitism and amensalism (Supplementary table IV). The opposite happens for *Proteobacteria*, whose species are more involved in parasitic associations than in neutralistic. *Spirochaetes*, *Verrucomicrobia* and *Ignavibacteria* among others, are the species interacting the most through mutualistic association, while *Caldiserica* and *Tenericutes* are frequently amensalistic (Supplementary table IV).

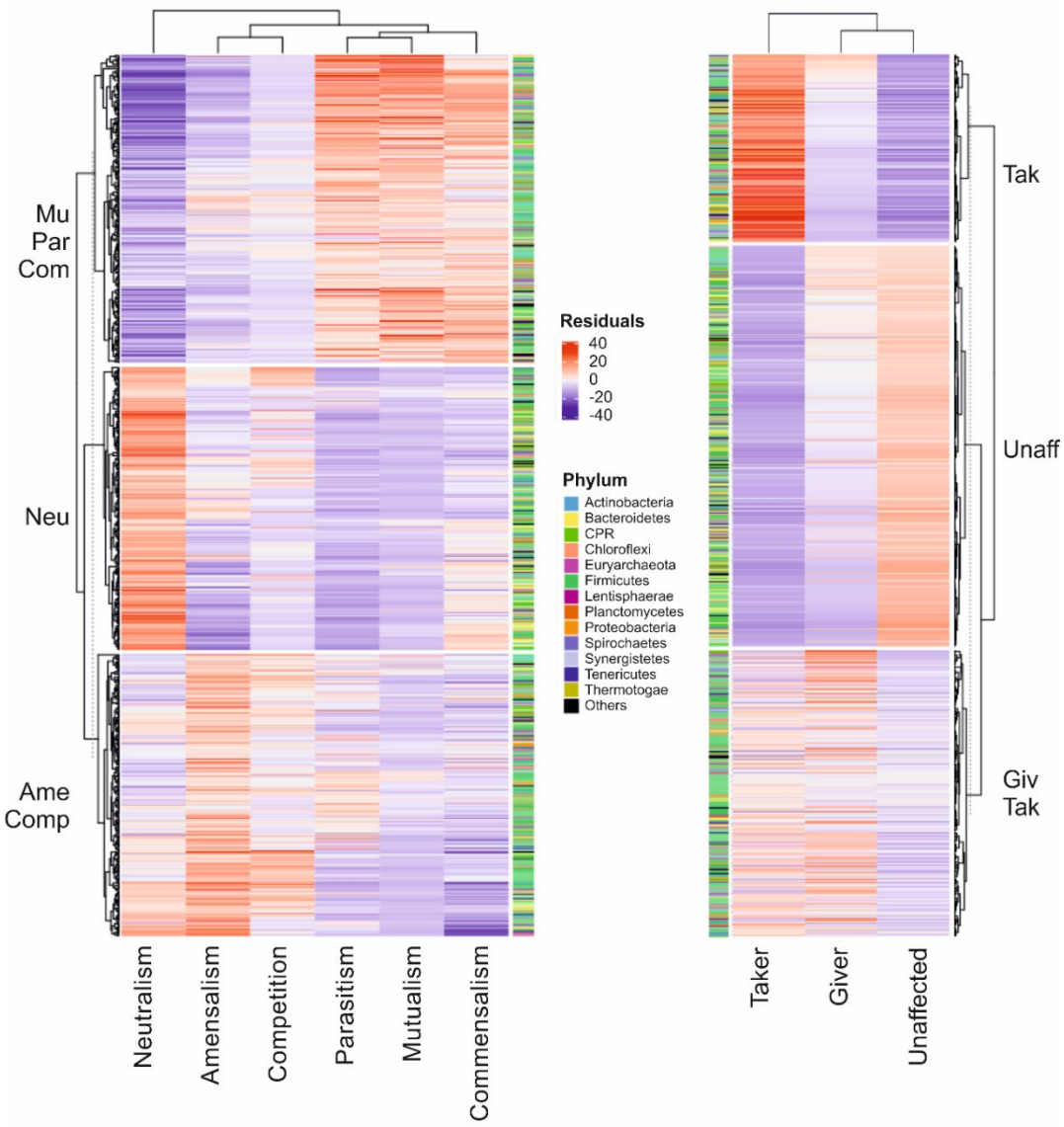

Fig. 2. Hierarchical clustering of the Pearson residual values.

Clustering has been performed both on interactivity and roles preferences profiles. The first highlights three main groups of species having different interactivity profiles. “Neu” includes species characterized mostly by neutralism and competition; “AmeComp” comprises those being predominantly amensalistic or competitive; “MuParCom” containing those that are primarily mutualistic, parasitic and commensalistic. Clustering of the residual values performed on interactivity roles was performed in order to evidence species behaving as “givers” or “takers”. Three main groups of species were identified: “Unaff” includes those correlated neither with “giver”, nor with “taker” behaviour (Neutral); “GivTak” consists of those with a heterogeneous behaviour in the interactions; “Tak” involving those behaving mainly as takers.

General preferences at species level were defined by hierarchical clustering identifying three main behavioural clusters (Fig. 2): Neu, for microbes with preference for neutralism, AmeComp, for microbes with preference for amensalism and competition, MuParCom, for microbes with preference for mutualism, parasitism and commensalism. *Euryarchaeota* are mostly associated with Neu and MuParCom, with *Methanosaeta* and *Methanomassiliicoccus* species belonging to Neu and *Methanothermobacter* and *Methanosarcina* species belonging to MuParCom (Fig. 2). This finding indicates that some archaeal species are more likely to express syntrophic behaviour. Among others, *Coprothermobacterota* were also mainly found in MuParCom, which could explain why *Methanothermobacter wolfeii* GSMM0047, *Methanothermobacter* sp. GSMM0492 and *Methanosarcina thermophila* GSMM0009 outcompete other archaea in the establishment of the community (Fontana et al., 2018). However, this behaviour was not limited to archaeal species, as the two dominant bacteria *Coprothermobacter proteolyticus* GSMM0002 and *Defluviitoga tunisiensis* GSMM0021 (up to 68% of combined relative abundance) adopted this behaviour too. Indeed, previous research performed on the metabolic pathways and the distribution of *D. tunisiensis* in the AD environment suggested that it can be involved in syntrophic associations and metabolic exchanges with hydrogenotrophic methanogens (Maus et al., 2016). Nevertheless, *D. tunisiensis* is able to grow in pure culture, suggesting that syntrophies are not obligatory, albeit fruitful (Campanaro et al., 2018).

Another example for the importance of positive syntrophies was given by the PA.IN. inspection of *Bifidobacterium crudilactis* GSMM0001. This microbe presented a neutral behaviour in only 16% of the pairs, while on average other microbes remained unaffected in 51% of the pairs. This result could explain its great abundance, reaching 85% in the acidogenic community. A random sampling-based permutation test (see subsection 4.4 for additional details) revealed that highly abundant species like *B. crudilactis* GSMM0001 tend to show an overall positive behaviour, while low abundant species prefer amensalism. In general, most *Bacteroidetes* fell into the AmeComp

cluster, and they were mainly unaffected by the interactions (growth rate variations were between -10% and 10%), indicating that these taxa use the same compounds as others, but without being outcompeted. The dominant biosphere is represented by a cooperative community conforming to the black queen hypothesis (Mas et al., 2016), while the rare microbes have overlapping nutritional requirements resulting in a more competitive community shaped as in the red queen hypothesis (Bonachela et al., 2017).

2.2 Microbial classification based on individual interaction role

Following the evaluation of microbial couples' behaviour during interactivity, it was possible to isolate and inspect the individual role of each microbe in the community by focusing on growth rate variations of the single species within each couple. In particular, the single microbes could benefit from the coexistence (takers) or were being negatively affected (givers). Species not influenced were defined as "unaffected". The significance of preferences for a specific role (givers or takers) was determined by chi-square statistics. Cluster analysis performed on residuals divided the species in three main clusters according to their behaviour (Fig. 2). Most abundant species were "takers" and included in the "Tak" cluster. This trend shows two relevant exceptions, i.e. the abundant species *D. tunisiensis* GSMM0021 and *Epulopiscium* sp. GSMM0167, both belonging to "GivTak". The rare biosphere was mainly included in cluster "Unaff", characterized by species with an unaffected behaviour (Neutral).

Interspecies interactions could involve members of different phyla (interphyla) or could occur within the same phylum (intraphylum) (Fig. 3). Bacteria exclusively involved in interphyla relationships mainly belonged to *Planctomycetes*, *Actinobacteria*, *Chloroflexi* and *Thermotogae*, while other phyla showed either "intra" or "interphyla" interactivity. Notably, intraphylum mutualism was very rare, representing less than 0.001% of the total number of cross-feedings identified for a specific phylum (Fig. 3A). Possibly, this surprising feature is due to the similarities in the metabolic properties of species belonging to the same phylum, which tend to be involved in the same "trophic

level" of the AD microbiome. This can result in species of the same phylum having a higher level of competition and a lower number of mutualistic crosstalks, which in turn were more frequent between microbes participating in different functional steps. On the contrary, amensalism can occur intraphylum, revealing a competitive behaviour between microbes of the same level contending for resources (Fig. 3B). The most prominent amensalistic tendency was observed between *Firmicutes* and *Caldiserica*, whilst *Firmicutes* and *Fusobacteria* had the strongest mutualistic relationships.

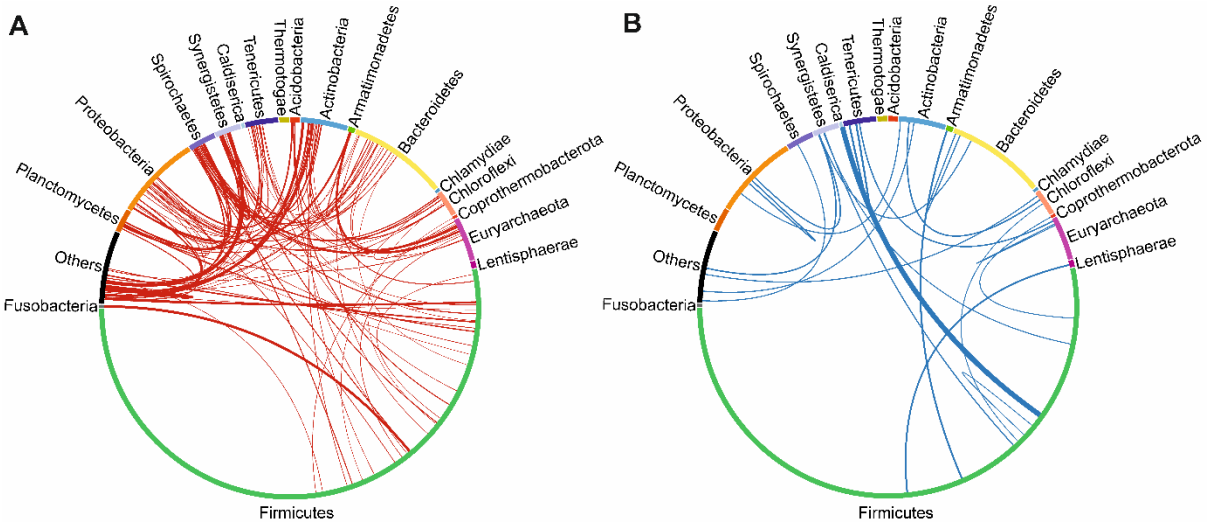

Fig. 3. Representation of interactions at phylum level.

(A) and (B) depict mutualistic and amensalistic interplays, respectively. Circumference arc length is proportional to the number of species in the corresponding phylum. Phyla represented by a low number of species were merged and named as "Others". Red (mutualistic) and blue (amensalistic) edge thickness represents the number of interplays normalized per phylum by number of species and having relative frequency higher than 0.001%.

2.3 Influence of externally supplied hydrogen on microbial interplay

Hydrogen injection resulted in an increased number of mutualistic and commensalistic cross-talks as well as in fewer negative and neutral influences (Fig. 4, Supplementary Table III), even though this effect was not widespread in the microbiome. In fact, despite the central role of hydrogen in many metabolic processes (it was present in

823 models and predicted to be exported by 509 species), its exogenous addition impacted only 4.33% of the interacting microbial couples. The cooperative tradeoff algorithm confirmed that hydrogen injection affects less than 5% of the couples and drives the community to a more cooperative behaviour (Supplementary Table III). Analyses performed in a methanogenic reactor supplemented with the feedstock simulated in the present study, revealed that relative abundances of *Leuconostoc* sp. GSMM0134 and *Pseudomonas lactis* GSMM0003 were markedly increased after H_2 injection (Fontana et al., 2018). Interestingly, PA.IN. results revealed that both microbes switched from negative to positive interactivity after H_2 addition. For instance, the growth of *Leuconostoc* sp. GSMM0134 before H_2 injection was negatively affected by 15 different members of the methanogenic community (of 22 in total), which were probably competing for substrates (e.g. lactose, serine) or taking advantage of by-products derived from substrate metabolism (e.g. L-Alanine, L-Arabinose, Diacetyl, Succinate) (Supplementary Table V). External hydrogen addition shifted this metabolic equilibrium, reducing the existing negative interactions to six and enhancing the average growth rate of *Leuconostoc* sp. GSMM0134 from 0.08 to 0.11 1/h. On the contrary, *P. lactis* GSMM0003 initially had a more diverse range of interaction types that changed significantly upon hydrogen addition. Its average growth rate increased slightly from 28.24 to 28.66 1/h and eight of its parasitic relationships became mutualistic or commensalistic, with other five commensalistic relationships shifting to parasitic (Supplementary table III). Although externally supplied H_2 influenced few selected couples, this finding suggests that changes induced remarkable improvements in the syntrophies between bacteria and, consequently, resulted in an increased methane production.

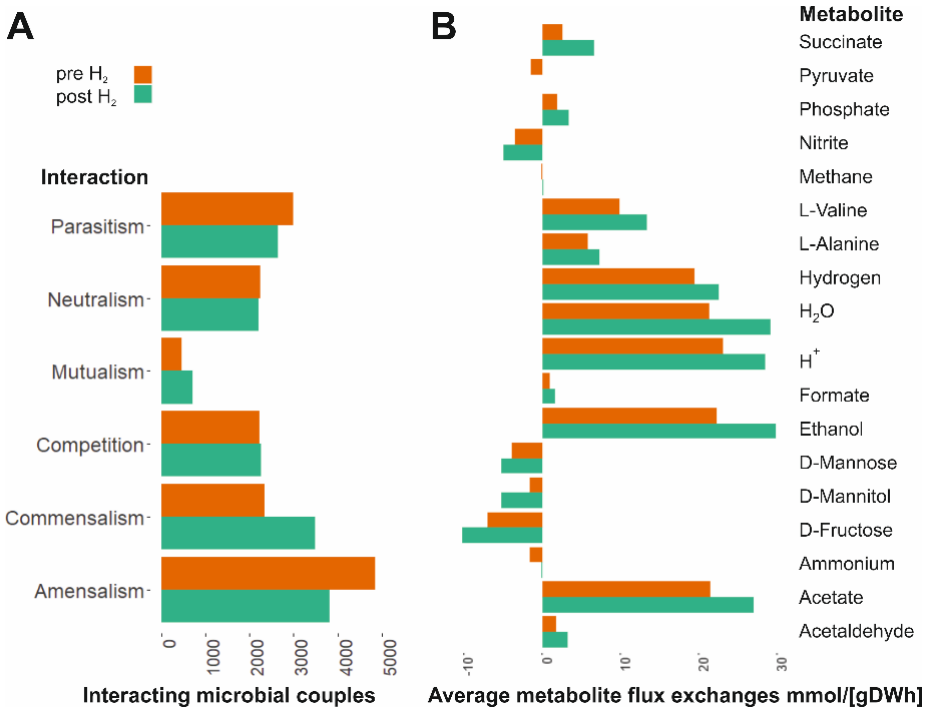

Fig. 4. Histograms representing the effect of H_2 injection on the community. (A), (B) effect on the microbiome interactivity profile and on average metabolite production/consumption respectively. In panel A, shown interactions are only those that change between the two conditions.

2.4 From a global inspection to a detailed view of the interactions

In order to substantiate and identify the interaction relations of the AD microcosms a second case study was investigated. It represents the AD microbiome, including metagenomic and metatranscriptomic data derived from the digestion of a simple substrate composed by sugars and proteins in a two stage system (Fontana et al., 2018). Microbial communities inhabiting one methanogenic and one acidogenic reactor were chosen in order to evaluate the compounds exchanged among species. In particular, this experiment is taken as a case of study since it holds a combination of features (i.e. small communities, high quality microbial genomes, simple feedstock) that make it ideal for flux balance simulations. All microbes having relative abundance greater than 0.01% in at least one of the two conditions were considered, representing 69 and 10 species in methanogenic and acidogenic communities respectively. The archaeal repertoire includes five species, one *Methanosarcina* (having the most

versatile metabolism), two *Methanothermobacter* and two *Methanoculleus* (pure hydrogenotrophs). The rest of the microbiome includes bacteria of *Actinobacteria*, *Bacteroidetes*, *Coprothermobacterota*, *Firmicutes*, *Proteobacteria*, *Synergistetes* and *Thermotogae*. Consistently with the experimental results, metabolite exchange simulations indicated 10% increase in butyrate and methane, and 5% in acetate production in the single-stage setup (methanogenic reactor). In the microbiome of acidogenic reactor (two-stage system), the repertoire includes only bacteria of the *Firmicutes*, *Proteobacteria* and *Actinobacteria* phyla and no archaea, due to the low pH (i.e. 3.9 ± 0.1) inhibiting the methanogenic process and hampering their growth. Here, the simulations showed an increase in butyrate and acetate production and a global increase of VFA, confirming previous findings about their importance. Furthermore, the computational approach also estimated differences in the production of several other compounds, which were not considered in the original study. In the methanogenic reactor, for example, a decrease in the production of acetaldehyde, (S)-propane-1,2-diol, pyruvate and ethanol was suggested by the simulations, following hydrogen injection. Conversely, the uptake of L-aspartate, glycine, D-alanine and L-glutamate was positively influenced subsequent to hydrogen injection (Supplementary Table V).

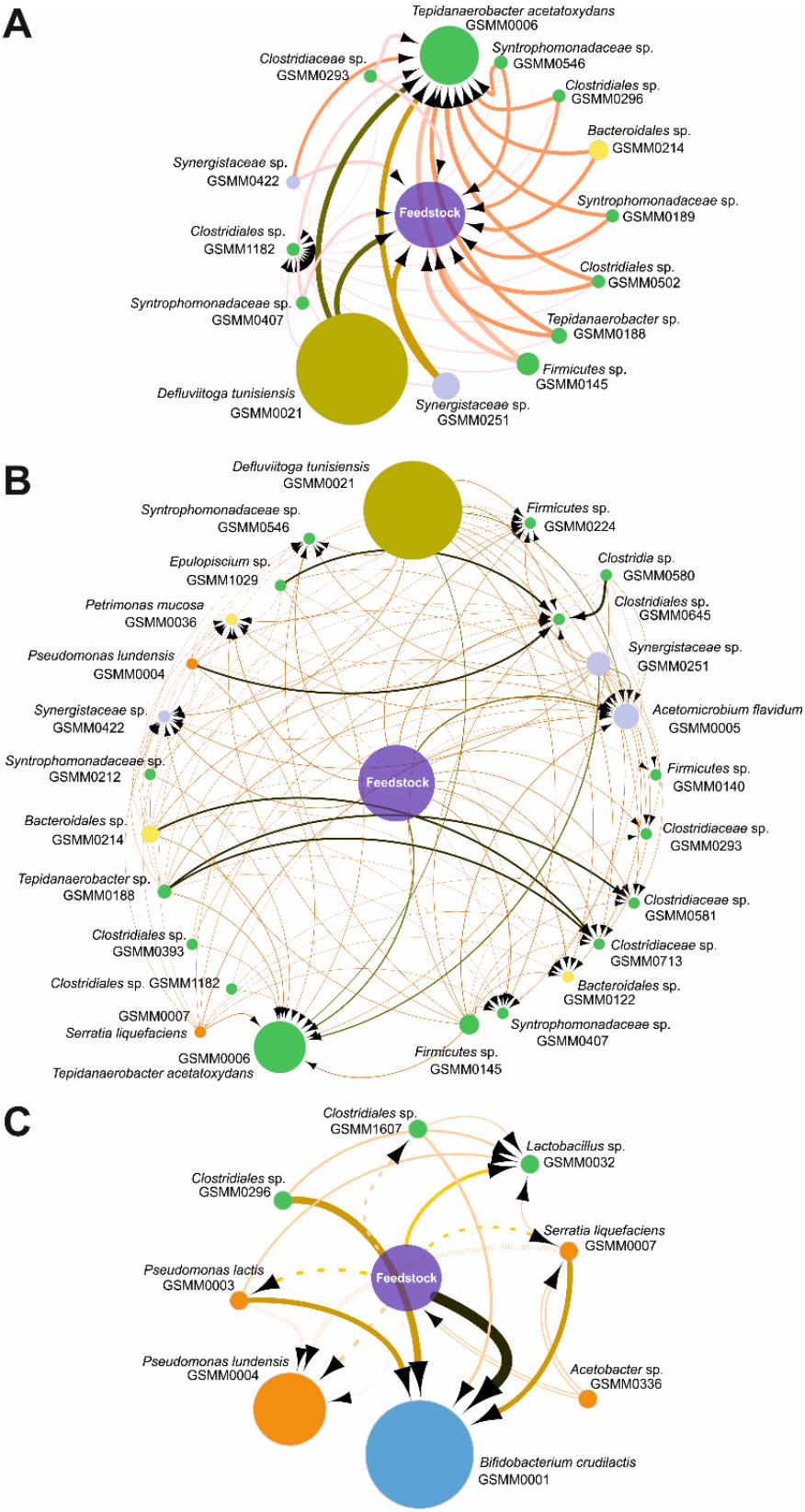

472

473 Fig. 5. Visualization of metabolic exchanges occurring between microbes present in the

474 reactor and / or with the medium.

A-C. Circles represent the single microbes, the diameter is proportional to the species abundance and the colour denotes the phylum. The medium is represented by the purple circle in the middle. Results for selected glucogenic amino acids such as glycine (A), and valine (B) are reported. In panel (C), key compounds related to the AD process, such as acetate (dashed lines), acetaldehyde (solid lines), formate (parallel lines) and hydrogen (vertical slashed lines), are shown. Arrows thickness is proportional to the fluxes between species. Exchanges occurring in the methanogenic (A-B) and in the acidogenic (C) reactors, respectively, are reported.

In order to verify a putative causal relationship between metabolic compound exchange and results obtained from microbial coexistence, a comparative analysis was performed. In the methanogenic reactor, out of 196 compounds exported by at least one of the microbes, only 58 (29.6%) could be imported by other species and were predicted as “cross feedings”. Among those, 18 metabolites were related to amino acid metabolism, to which a similar prediction was evidenced in other complex microbial communities by Parks and colleagues (Parks et al., 2017). Amino acid interdependence is strictly linked with the lack of TCA cycle intermediates (Thommes et al., 2019). However, this imbalance, causing auxotrophies, can be compensated by compounds exchanges between members of the community. Metabolic exchange (ME) analysis (see subsection 4.3 for additional details) underlined the relevant role of glucogenic amino acids such as glycine, valine, and glutamate in the AD microbiome (Fig. 5). These compounds can be converted into intermediates of the TCA cycle, like glycine, the precursor of pyruvate, which is then converted into acetyl-CoA. Other compounds, such as valine and glutamate, are respectively precursors of succinyl-CoA and alpha-ketoglutarate.

According to the FBA carried out on the microbial community growing in the methanogenic reactor, *Defluviitoga tunisiensis* GSMM0021 was the most efficient producer of glycine and valine (Fig. 5A, Fig. 5B and Supplementary Table V), as well as the most abundant species. *Tepidanaerobacter acetatoxydans* GSMM0006 was

predicted as the main up-taker of the two metabolites and the second most abundant microbe. Additionally, *P. lundensis* GSMM0004 produced L-proline, which was imported by *B. crudilactis* GSMM0001 and converted into alpha-ketoglutarate. Another potential syntrophy was found between *Lactobacillus paracasei* subsp. *paracasei* GSMM0008 that produced L-Valine, and *Leuconostoc* sp. that imported and converted it to succinyl-CoA (Fig. 6). Both alpha-ketoglutarate and succinyl-CoA are TCA cycle intermediates and can be transformed into adenosine triphosphate (ATP), carbon dioxide and the reducing agent NADH (Moat et al., 2002). This finding hints the presence of a meta-communication, which is relevant also in the acidogenic reactor.

Another interesting result obtained from ME revealed that a simultaneous exchange of acetaldehyde and acetate was occurring in the acidogenic reactor (Fig. 5C). *Serratia liquefaciens* GSMM0007, *P. lactis* GSMM0003 and *Clostridiales* sp. GSMM1607 were the major up-takers of acetaldehyde and the main producers of acetate, implying that the latter compound is generated by the activity of acetaldehyde dehydrogenase in specific bacteria. *B. crudilactis* GSMM0001 was the most abundant microbe overall, absorbing the vast majority of acetaldehyde and hydrogen, and concurrently stressing the key role of these compounds for the proper functioning of the acidogenic reactor.

A putative syntrophic association between *Coprothermobacter proteolyticus* GSMM0002 and *Methanothermobacter wolfeii* GSMM0047 was previously proposed (Fontana et al., 2018). Considering the relevance of this syntrophy in the methanogenic process, it was chosen for a detailed analysis, using the new methodology developed and supported by RNA-seq data integration. Previous studies mentioned a cooperative coexistence between proteolytic anaerobic bacteria and hydrogen-converting methanogens, evidencing that this syntrophy can lead to an increased cell growth and a better degradation efficiency (Stams, 1994). The present analysis showed that the two species could indeed reciprocally influence the growth rate of one another, with *C. proteolyticus* GSMM0002 benefiting from this relationship in both conditions analysed and *M. wolfeii* GSMM0047 remaining almost unaffected. Furthermore, ME showed that *C. proteolyticus* GSMM0002 produced H_2 and iron

(Fe^{2+}), which were subsequently used by *M. wolfeii* GSMM0047, partially in agreement with FBA integrating simulation of population steady-state metabolism (Supplementary Table III). However, a comparative evaluation performed with ME and starting from the results obtained with PA.IN. revealed a more complex situation. Both *C. proteolyticus* GSMM0002 and *M. wolfeii* GSMM0047 benefited from the presence of several other *Clostridiales* species in commensalistic interactions. *M. wolfeii* GSMM0047 obtained H_2 and formate from *Clostridiales* species, while *C. proteolyticus* GSMM0002 absorbed tryptophan, L-proline and L-isoleucine, which are precursors of alpha-ketoglutarate: a compound with a key role in the TCA cycle (Niehaus et al., 2019). Above result was supported by previous work asserting that SAOB interplays are not simply dualistic as previously thought but are based on multiple cross-feeding effects (Westerholm et al., 2019). Finally, the original study reported an increase in methane production after H_2 injection, and proposed an archaeal species potentially responsible for the biogas upgrading process (Fontana et al., 2018). In support of this proposal, ME estimated that *Methanoculleus thermophilus* GSMM0046 was the microbe that profited the most from injecting H_2 in the reactors, establishing it as the main microbe responsible for the increased methane yield and purity. These results were confirmed by simulations implementing gene expression values used to constrain the solution space (Supplementary Table V). For example, the flux for methane production shifts from 111.73 to 396.35 mmol/[gDWh], indicating an increase subsequent to H2 addition. However, based on the simulations integrating steady-state metabolism, *M. thermophilus* GSMM0046 showed strong profiteer behaviour, further emphasised after additional hydrogen injection (Supplementary Table III). In particular, parasitic relationships may be due to an enhanced uptake of several key metabolites and co-factors (Appendix, Table S2) by the archaeon. These compounds, thus, resulted less available in the medium for the other members of the community.

Since there is not a universally accepted method to perform MFB community simulations and due to potential biases of the different approaches, some discrepancies are expected; however the key patterns obtained are in agreement and

support the findings both at coarse and fine grain level related to main behaviour of the AD microbiome.

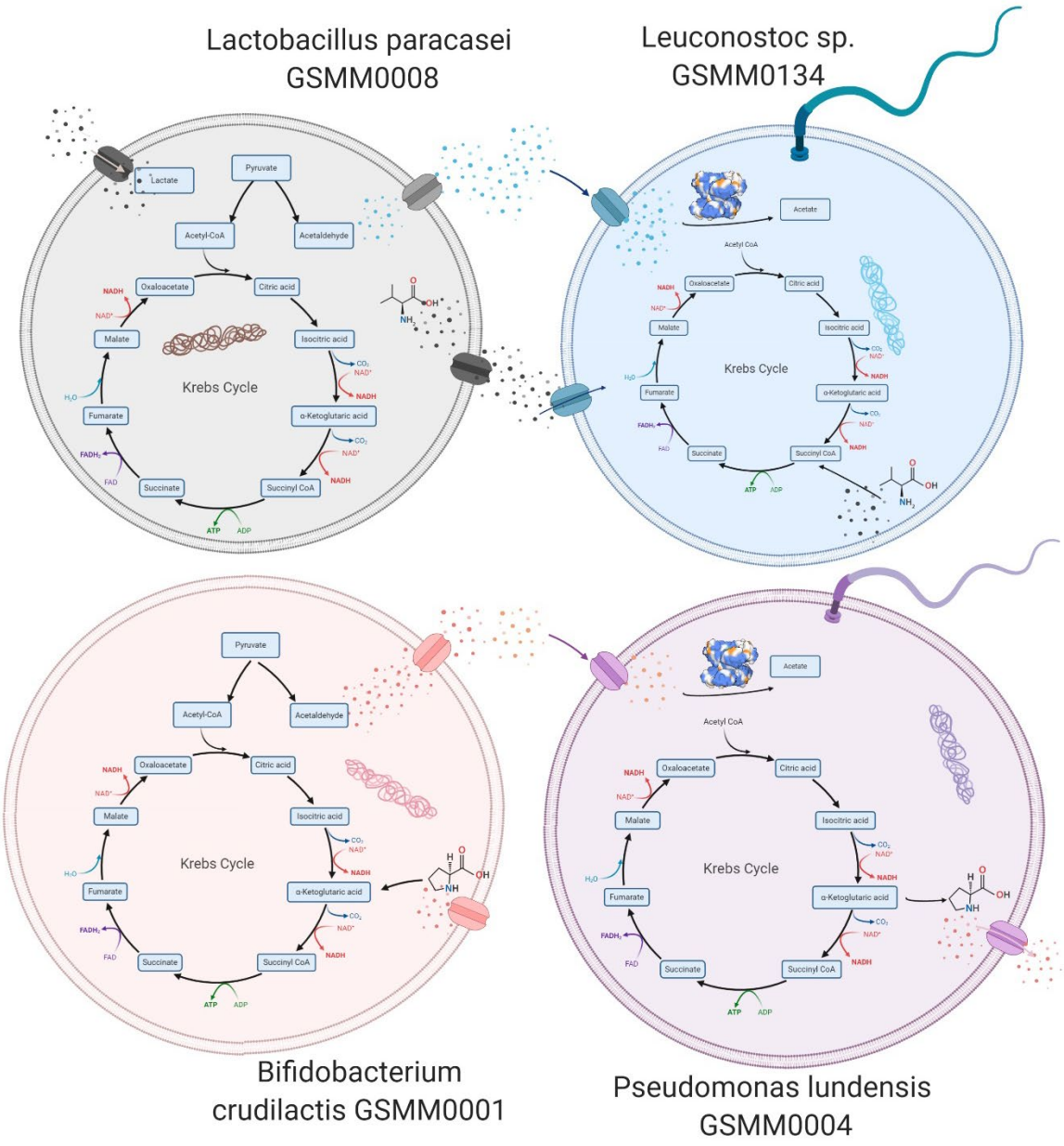

Fig. 6. Schematic representation of the TCA cycle in the four dominant species present in the acidogenic reactor.

Results were integrated with the predicted amino acids exchanges influencing the TCA cycle. The enzymatic structure represents the acetaldehyde dehydrogenase performing the conversion of acetaldehyde into acetate.

3. Conclusions

The major novelty of the current study is the combination of metabolic reconstruction and modelling across hundreds of species for the detection of molecular mechanisms behind their interactions at an unprecedented level of detail. To our knowledge, this is the first attempt to massively generate models from high-quality MAGs, and to use flux balance analysis for the inspection of a complex biologically mediated biogas production system. The generation of metabolic models derived from known species, and identified in the environment by means of 16S rRNA similarity search, leaves unresolved questions due to the presence of uncultivated microbes. On the contrary, the approach proposed here paves the way to the use of FBA in the functional investigation of the microbiome and allows a deeper understanding of all the species present. The investigation of pairwise influence provided a comprehensive overview of the microbial community involved in the anaerobic digestion process. From the present investigation it emerges that reciprocal influence in the microbial growth rate can be calculated in-silico and largely depends on competition/sharing for/of metabolites. The used approach was successful in picking out strong differences in interactivity roles between species that became prevailing in the community evidencing how in this ecosystem two kinds of complementary communities coexist. The consortium in the AD subsystem is stabilized by syntrophies and auxotrophies. The accuracy of model creation and medium characterization enabled the identification of key metabolites fluctuations between two experimental conditions characterized by H_2 injection. This resulted in differences in microbial growth correlated with specific feedstock compositions. This analysis suggests that investigation of pairwise interactivity can help in providing fundamental insights into complex microbial populations (Weinrich et al., 2019). This approach is shedding light on the network occurring in the AD “black-box” and paves the way to a functional prediction of the AD microbiome based on FBA. In perspective this newly developed

procedure can target biogas production improvement through the design of “ad hoc” microbial consortia or by predicting substrate effects on the microbiome dynamics.

4. Material and Methods

4.1 Description of the experiments

For carrying out the modelling work and validating the metabolic models used in the present study, MAGs were obtained from the comparative analysis recently published by Campanaro (Campanaro et al., 2020). The comparative analysis of more than 130 publicly available experiments from a range of Anaerobic Digestion engineered systems enabled the reconstruction of 5400 MAGs clustered into 1’600 different species with 837 of them identified as high quality according to MIMAG guidelines. This repertoire is available in the database http://microbial-genomes.org/projects/biogasmicrobiome. From this dataset only 836 MAGs, identified as “high quality” regarding their genome completeness and contamination according to MIMAG guidelines (Bowers et al., 2017), have been considered for genome-scale metabolic model (GSMMs) reconstruction.

A comparison of single and two-stage AD setups was used from an earlier publication (Fontana et al., 2018) included in the dataset mentioned above. The single stage reactor characterizes a complete AD process fed with a mixed substrate of cheese whey and residues from cheese processing. On the other hand, the second system was composed of two reactors: the first reactor was fed as in the single-stage setup and used for the acidogenic step of AD, while its effluent was fed to the second reactor where methanogenesis took place. Both reactor systems had an operating temperature of 55±1 °C and were run without and with H_2 injection (period I and II, respectively), in order to evaluate whether the injection of H_2 modified the methane yield. For the present analysis, only the microbial communities from the methanogenic step of the single reactor and from the acidogenic step of the two-stage reactor setup were considered. The communities taken into account consisted of species having

relative abundances higher than 0.01% in at least one of the four conditions analysed (acidogenic of the two stage and methanogenic steps of the single stage setup, with and without H_2 injection), following (Fontana et al., 2018).

4.2 Genome-scale metabolic reconstruction and modelling of the anaerobic digestion community

A tutorial was realized specifically for the replication of the analysis described in the present study (https://github.com/arianccbasile/ADinteractions).

Starting from quality-filtered MAGs, the genome scale metabolic models (GSMMs) for the corresponding species were created with CarveMe v. 1.2. 1 (Machado et al., 2018) using for each microbe the most appropriate universe (grampos, gramneg or archaea) according to its taxonomy and the default gene matching parameters. The typical top-down reconstruction approach implemented in CarveMe generated models with standardized molecular weight of the biomass product. This is crucial, because without proper normalization, hidden biases in biomass molecular weight can generate significant simulation discrepancies (Siu H.J. Chan et al., 2017).

The solver used for GSMM reconstruction is Cplex (v. 12.8.0.0) (IBM, 2019). Sanity checks were performed on all the metabolic models, testing twelve basic properties through the COBRA toolbox (Brunk et al., 2018; Heirendt et al., 2019). Moreover, the consistency of all models was systematically assessed through the standardized MEMOTE test suite (Lieven et al., 2020). Since AGORA (assembly of gut organisms through reconstruction and analysis) models represent a golden standard in the field of large-scale metabolic reconstructions, the analysis has been performed both on our models and on AGORA models (Magnúsdóttir et al., 2017) to inspect the main differences. To test the soundness of the models, the presence and completeness of their pathways associated to carbohydrate and lipid metabolism have been verified by considering the cross references in the microbial models and tracking the presence of specific reactions. Completeness of the KEGG modules was assessed for those belonging to carbohydrate and lipid metabolism. For the inspection of methanogenesis

and the Wood–Ljungdahl pathway (syntrophic acetate oxidation and/or acetogenesis), a manual validation of all the reactions was performed, taking into account relevant information derived from literature for the known species. Composition of the media has been obtained from the nutrition resource of the Virtual Metabolic Human database considering the following food entries: “Whey, acid, fluid”, “Whey, acid, dried”, “Whey, sweet, fluid”, “Whey, sweet, dried”. The corresponding exchange reactions have been refined through a manual work based on the experimental data previously reported (Fontana et al., 2018). The media composition is thoroughly described in the dedicated github. The medium composition was integrated in the model as nutrient constraints modifying accordingly the upper and lower bounds of export reactions through an in-house developed function (“apply_diet” in the github).

4.3 Modelling of biological and metabolic interactions

The analysis of the interactions among the different microbes was inferred using FBA. For the current analysis Python and the COBRApy library (v. 0.17.1) (Ebrahim et al., 2013) were used. In order to use the metabolic models generated with CarveMe (v. 1.2.1), and to use the code with multiple processors the original MMinte (v. 1.0.3) (Mendes-Soares et al., 2016) code was adapted and reported in github as PA.IN. The generation of the communities follows the approach used in MMinte for the creation of multi-species stoichiometric models. This approach introduces a fictitious compartment that represents the extracellular environment shared by both species, and adds reactions allowing metabolites that are imported or secreted by each individual species to be transformed into community metabolites. Singular growth outcomes were computed by maximizing for total biomass production, setting the maximal community growth as the objective function assuming that even for parasitic or competitive microbes the best outcome is the maximal growth of the couple. The growth rates for each species under defined nutrient conditions is estimated in isolation and in the presence of another species, by running FBA in COBRApy. The algorithm simultaneously maximizes for the biomass objective function of both

GSMMs for the estimation of the growth rate of each species when coexisting with the other. The algorithm then knocks out all reactions of one species whilst maximizing the biomass objective function of the other to simulate the growth rate of each species individually. In this step the solver used is Glpk (Oki, 2012). A difference in the growth rate of ±10% or more for at least a pair member, compared with the growth rate of the microbes grown separately, was considered significant to define the presence of an interaction. By comparing the growth rate of each microbe when coupled with another, it was possible to distinguish six different types of interaction: parasitism, commensalism, neutralism, amensalism, competition and mutualism. If at least one of the two species was negatively affected by the interaction, the interplay was classified as negative, otherwise as positive. In some of these scenarios (namely Parasitism, Commensalism and Amensalism) each of the two species was classified either as a "giver" or a "taker", depending on the impact of the pairing on their growth.

Interactions among the dominant members of the biosphere were verified using the cooperative tradeoff algorithm of Micom (v.0.10.1) (Diener et al., 2020), an approach mimicking the strategy implemented in OptCom (Zomorrodi and Maranas, 2012). By using this algorithm the individual growth is simultaneously at its maximum rate without diminishing the growth rate of other individuals (thus the term "cooperative"). Analysis of the metabolic exchanges among the different microbes has also been performed using MICOM integrating in the community model the microbial abundance as well and modifying the boundaries of the models according to the medium with an in-house developed script ("apply_diet" in the dedicated github). For each microbial pair, metabolite exchange rates were estimated through parsimonious FBA (Lewis et al., 2010) by setting the community biomass accumulation as objective. In this step, the solver used was Gurobi (v. 8) (Inc., 2014). Results were converted in tabular format and used to generate inputs file for Cytoscape software (3.2.1) (Demchak et al., 2014). Graphical representation of metabolic exchanges was performed with Cytoscape to simplify the interpretation of MICOM results.

Metatranscriptomic data of twelve samples obtained from Fontana et al. (2018) were added to the simulation. Details of RNA extraction and standard raw RNA-seq data processing have been previously reported (Fontana et al., 2018). Gene expression analysis was performed using as reference the MAGs previously identified (Campanaro et al., 2020). Gene finding was performed using Prodigal (v2.6.2) (Hyatt et al., 2010) and reported in a previous study (Campanaro et al., 2020). RNA-seq reads were aligned on reference metagenome assembly using bowtie2 (v2.2.4) (Langmead and Salzberg, 2012) and the number of reads mapped per each gene was determined from the "bam" file using SeqMonk (v1.45.4) (Anders et al., 2015) using the options "opposing strand specific" and "apply transcript length correction". The metatranscriptomic data were implemented in the metabolic models as constraints readapting the code of METRADE (Angione and Lió, 2015) to the multispecies pairwise communities. Metabolic exchanges obtained starting from models with inner constraints derived from metatranscriptomic data were analysed as before. Metabolic models were deposited in the public repository figshare (10.6084/m9.figshare.12661496.v1).

Finally, we compared our results on metabolic exchanges obtained by Micom with those obtained through SteadyCom, a different approach for metabolic community modelling (Siu Hung Joshua Chan et al., 2017). In the SteadyCom simulations, the medium was integrated as microaerophilic, setting the aggregate oxygen uptake bound to 0.1 mmol/h, upon finding that a completely anaerobic environment prevents most species from growing in isolation.

4.4 Statistical analyses

All the statistical analyses were carried out with R software v.3.5.2 (Breuer, 2017). The χ^2 test of Independence to characterise bacterial interactions across species was accomplished with chisq.test in the package stats. Pearson's residuals were obtained from the same function. Hierarchical clustering was applied via the ComplexHeatmap package (Gu et al., 2016), employing a squared Euclidean distance of the values

between the 10th and the 90th percentile, thereby eliminating the influence of the outliers (Appendix, Supplementary Methods, robust_dist). To verify the different interactivity profile of abundant and rare community members, a permutation test was carried out through the R base “sample” function, generating 2000 random permutations (Appendix, Supplementary Methods, casual_campioning).

Acknowledgements

This work was financially supported by the “Budget Integrato della Ricerca Dipartimentale" (BIRD198423) PRID 2019 of the Department of Biology of the University of Padua, entitled “SyMMoBio: inspection of Syntrophies with Metabolic Modeling to optimize Biogas Production”. The PhD fellowship of AB is supported by “Progetto di Eccellenza DiBio” of University of Padua. Authors want to thank Emiliano Ciuffa for his significant contribution on linguistic revision of the manuscript and Daniel Machado for the important suggestions provided during the revision process. A final acknowledge to the Italian Consortium for Biotechnologies (CIB) for the support.

Author contributions

AB, LT and SC conceived the experimental project; AB designed most of the experimental strategy, developed code for the modelling analysis and performed the statistical analysis. All the authors wrote and revised the manuscript.

Conflicts of interest

The authors declare that they have no conflict of interest.

References

760 Ahring, B.K., Sandberg, M., Angelidaki, I., 1995. Volatile fatty acids as indicators of
761 process imbalance in anaerobic digestors. Appl. Microbiol. Biotechnol. 43, 559–
762 565. https://doi.org/10.1007/BF00218466
763 Anders, S., Pyl, P.T., Huber, W., 2015. HTSeq-A Python framework to work with high-
764 throughput sequencing data. Bioinformatics 31, 166–169.
765 https://doi.org/10.1093/bioinformatics/btu638
766 Angelidaki, I., Treu, L., Tsapekos, P., Luo, G., Campanaro, S., Wenzel, H., Kougias,
767 P.G., 2018. Biogas upgrading and utilization: Current status and perspectives.
768 Biotechnol. Adv. https://doi.org/10.1016/j.biotechadv.2018.01.011
769 Angione, C., Lió, P., 2015. Predictive analytics of environmental adaptability in multi-
770 omic network models. Sci. Rep. https://doi.org/10.1038/srep15147
771 Bonachela, J.A., Wortel, M.T., Stenseth, N.C., 2017. Eco-evolutionary Red Queen
772 dynamics regulate biodiversity in a metabolite-driven microbial system. Sci. Rep.
773 7. https://doi.org/10.1038/s41598-017-17774-4
774 Boon, E., Meehan, C.J., Whidden, C., Wong, D.H.J., Langille, M.G.I., Beiko, R.G.,
775 2014. Interactions in the microbiome: Communities of organisms and
776 communities of genes. FEMS Microbiol. Rev. https://doi.org/10.1111/1574-
777 6976.12035
778 Bowers, R.M., Kyrpides, N.C., Stepanauskas, R., Harmon-Smith, M., Doud, D.,
779 Reddy, T.B.K., Schulz, F., Jarett, J., Rivers, A.R., Eloe-Fadrosh, E.A., Tringe,
780 S.G., Ivanova, N.N., Copeland, A., Clum, A., Becraft, E.D., Malmstrom, R.R.,
781 Birren, B., Podar, M., Bork, P., Weinstock, G.M., Garrity, G.M., Dodsworth, J.A.,
782 Yooseph, S., Sutton, G., Glöckner, F.O., Gilbert, J.A., Nelson, W.C., Hallam, S.J.,
783 Jungbluth, S.P., Ettema, T.J.G., Tighe, S., Konstantinidis, K.T., Liu, W.T., Baker,
784 B.J., Rattei, T., Eisen, J.A., Hedlund, B., McMahon, K.D., Fierer, N., Knight, R.,
785 Finn, R., Cochrane, G., Karsch-Mizrachi, I., Tyson, G.W., Rinke, C., Lapidus, A.,
786 Meyer, F., Yilmaz, P., Parks, D.H., Eren, A.M., Schriml, L., Banfield, J.F.,
787 Hugenholtz, P., Woyke, T., 2017. Minimum information about a single amplified
788 genome (MISAG) and a metagenome-assembled genome (MIMAG) of bacteria

and archaea. Nat. Biotechnol. https://doi.org/10.1038/nbt.3893

Breuer, J., 2017. R (Software), in: The International Encyclopedia of Communication Research Methods. pp. 1–2. https://doi.org/10.1002/9781118901731.iecrm0201

Brunk, E., Sahoo, S., Zielinski, D.C., Altunkaya, A., Dräger, A., Mih, N., Gatto, F., Nilsson, A., Preciat Gonzalez, G.A., Aurich, M.K., Prlic, A., Sastry, A., Danielsdottir, A.D., Heinken, A., Noronha, A., Rose, P.W., Burley, S.K., Fleming, R.M.T., Nielsen, J., Thiele, I., Palsson, B.O., 2018. Recon3D enables a three-dimensional view of gene variation in human metabolism. Nat. Biotechnol. 36, 272–281. https://doi.org/10.1038/nbt.4072

Budinich, M., Bourdon, J., Larhlimi, A., Eveillard, D., 2017. A multi-objective constraint-based approach for modeling genome-scale microbial ecosystems. PLoS One 12. https://doi.org/10.1371/journal.pone.0171744

Campanaro, S., Treu, L., Kougias, P.G., De Francisci, D., Valle, G., Angelidaki, I., 2016. Metagenomic analysis and functional characterization of the biogas microbiome using high throughput shotgun sequencing and a novel binning strategy. Biotechnol. Biofuels 9. https://doi.org/10.1186/s13068-016-0441-1

Campanaro, S., Treu, L., Kougias, P.G., Luo, G., Angelidaki, I., 2018. Metagenomic binning reveals the functional roles of core abundant microorganisms in twelve full-scale biogas plants. Water Res. 140, 123–134. https://doi.org/10.1016/j.watres.2018.04.043

Campanaro, S., Treu, L., Rodriguez-R, L.M., Kovalovszki, A., Ziels, R.M., Maus, I., Zhu, X., Kougias, P.G., Basile, A., Luo, G., Schlüter, A., Konstantinidis, K.T., Angelidaki, I., 2020. New insights from the biogas microbiome by comprehensive genome-resolved metagenomics of nearly 1600 species originating from multiple anaerobic digesters. Biotechnol. Biofuels. https://doi.org/10.1186/s13068-020-01679-y

Chaffron, S., Rehrauer, H., Pernthaler, J., Von Mering, C., 2010. A global network of coexisting microbes from environmental and whole-genome sequence data. Genome Res. 20, 947–959. https://doi.org/10.1101/gr.104521.109

Chan, Siu H.J., Cai, J., Wang, L., Simons-Senftle, M.N., Maranas, C.D., 2017. Standardizing biomass reactions and ensuring complete mass balance in genome-scale metabolic models. Bioinformatics 33, 3603–3609. https://doi.org/10.1093/bioinformatics/btx453

Chan, Siu Hung Joshua, Simons, M.N., Maranas, C.D., 2017. SteadyCom: Predicting microbial abundances while ensuring community stability. PLoS Comput. Biol. 13. https://doi.org/10.1371/journal.pcbi.1005539

Chow, D., Nunalee, M.L., Lim, D.W., Simnick, A.J., Chilkoti, A., 2008. Peptide-based biopolymers in biomedicine and biotechnology. Mater. Sci. Eng. R Reports. https://doi.org/10.1016/j.mser.2008.04.004

Clemente, J.C., Ursell, L.K., Parfrey, L.W., Knight, R., 2012. The impact of the gut microbiota on human health: An integrative view. Cell. https://doi.org/10.1016/j.cell.2012.01.035

Dailey, H.A., Gerdes, S., Dailey, T.A., Burch, J.S., Phillips, J.D., 2015. Noncanonical coproporphyrin-dependent bacterial heme biosynthesis pathway that does not use protoporphyrin. Proc. Natl. Acad. Sci. U. S. A. 112, 2210–2215. https://doi.org/10.1073/pnas.1416285112

Demchak, B., Hull, T., Reich, M., Liefeld, T., Smoot, M., Ideker, T., Mesirov, J.P., 2014. Cytoscape: The network visualization tool for GenomeSpace workflows. F1000Research 3. https://doi.org/10.12688/f1000research.4492.1

Diener, C., Gibbons, S.M., Resendis-Antonio, O., 2020. MICOM: Metagenome-Scale Modeling To Infer Metabolic Interactions in the Gut Microbiota. mSystems 5. https://doi.org/10.1128/msystems.00606-19

Ebrahim, A., Lerman, J.A., Palsson, B.O., Hyduke, D.R., 2013. COBRApy: COnstraints-Based Reconstruction and Analysis for Python. BMC Syst. Biol. 7. https://doi.org/10.1186/1752-0509-7-74

Faith, J.J., 2015. Bridging the knowledge gap: from microbiome composition to function. Mol. Syst. Biol. 11, 793. https://doi.org/10.15252/msb.20156045

Fontana, A., Kougias, P.G., Treu, L., Kovalovszki, A., Valle, G., Cappa, F., Morelli, L.,

847 Angelidaki, I., Campanaro, S., 2018. Microbial activity response to hydrogen
848 injection in thermophilic anaerobic digesters revealed by genome-centric
849 metatranscriptomics. Microbiome 6. https://doi.org/10.1186/s40168-018-0583-4
850 Gu, Z., Eils, R., Schlesner, M., 2016. Complex heatmaps reveal patterns and
851 correlations in multidimensional genomic data. Bioinformatics 32, 2847–2849.
852 https://doi.org/10.1093/bioinformatics/btw313
853 Hall, D.O., Scrase, J.I., 1998. Will biomass be the environmentally friendly fuel of the
854 future?, in: Biomass and Bioenergy. pp. 357–367. https://doi.org/10.1016/S0961-
855 9534(98)00030-0
856 Hay, M.E., Parker, J.D., Burkepile, D.E., Caudill, C.C., Wilson, A.E., Hallinan, Z.P.,
857 Chequer, A.D., 2004. Mutualisms and aquatic community structure: The enemy
858 of my enemy is my friend. Annu. Rev. Ecol. Evol. Syst.
859 https://doi.org/10.1146/annurev.ecolsys.34.011802.132357
860 Heinken, A., Thiele, I., 2015. Anoxic conditions promote species-specific mutualism
861 between gut microbes In Silico. Appl. Environ. Microbiol. 81, 4049–4061.
862 https://doi.org/10.1128/AEM.00101-15
863 Heirendt, L., Arreckx, S., Pfau, T., Mendoza, S.N., Richelle, A., Heinken, A.,
864 Haraldsdóttir, H.S., Wachowiak, J., Keating, S.M., Vlasov, V., Magnusdóttir, S.,
865 Ng, C.Y., Preciat, G., Žagare, A., Chan, S.H.J., Aurich, M.K., Clancy, C.M.,
866 Modamio, J., Sauls, J.T., Noronha, A., Bordbar, A., Cousins, B., El Assal, D.C.,
867 Valcarcel, L. V., Apaolaza, I., Ghaderi, S., Ahookhosh, M., Ben Guebila, M.,
868 Kostromins, A., Sompairac, N., Le, H.M., Ma, D., Sun, Y., Wang, L., Yurkovich,
869 J.T., Oliveira, M.A.P., Vuong, P.T., El Assal, L.P., Kuperstein, I., Zinovyev, A.,
870 Hinton, H.S., Bryant, W.A., Aragón Artacho, F.J., Planes, F.J., Stalidzans, E.,
871 Maass, A., Vempala, S., Hucka, M., Saunders, M.A., Maranas, C.D., Lewis, N.E.,
872 Sauter, T., Palsson, B., Thiele, I., Fleming, R.M.T., 2019. Creation and analysis
873 of biochemical constraint-based models using the COBRA Toolbox v.3.0. Nat.
874 Protoc. https://doi.org/10.1038/s41596-018-0098-2
875 Hyatt, D., Chen, G.L., LoCascio, P.F., Land, M.L., Larimer, F.W., Hauser, L.J., 2010.

876 Prodigal: Prokaryotic gene recognition and translation initiation site identification.
877 BMC Bioinformatics 11. https://doi.org/10.1186/1471-2105-11-119
878 IBM, 2019. CPLEX Optimizer [WWW Document]. Ibm. URL https://www.ibm.com/dk-
879 da/analytics/cplex-optimizer
880 Inc., G.O., 2014. Gurobi Optimizer reference manual. Www.Gurobi.Com 6, 572.
881 Jacobi, H.F., Moschner, C.R., Hartung, E., 2009. Use of near infrared spectroscopy in
882 monitoring of volatile fatty acids in anaerobic digestion. Water Sci. Technol. 60,
883 339–346. https://doi.org/10.2166/wst.2009.345
884 Jing, Y., Campanaro, S., Kougias, P., Treu, L., Angelidaki, I., Zhang, S., Luo, G., 2017.
885 Anaerobic granular sludge for simultaneous biomethanation of synthetic
886 wastewater and CO with focus on the identification of CO-converting
887 microorganisms. Water Res. 126, 19–28.
888 https://doi.org/10.1016/j.watres.2017.09.018
889 Jousset, A., Bienhold, C., Chatzinotas, A., Gallien, L., Gobet, A., Kurm, V., Küsel, K.,
890 Rillig, M.C., Rivett, D.W., Salles, J.F., Van Der Heijden, M.G.A., Youssef, N.H.,
891 Zhang, X., Wei, Z., Hol, G.W.H., 2017. Where less may be more: How the rare
892 biosphere pulls ecosystems strings. ISME J.
893 https://doi.org/10.1038/ismej.2016.174
894 Kanehisa, M., Sato, Y., Kawashima, M., Furumichi, M., Tanabe, M., 2016. KEGG as
895 a reference resource for gene and protein annotation. Nucleic Acids Res. 44,
896 D457–D462. https://doi.org/10.1093/nar/gkv1070
897 Keseler, I.M., Mackie, A., Santos-Zavaleta, A., Billington, R., Bonavides-Martínez, C.,
898 Caspi, R., Fulcher, C., Gama-Castro, S., Kothari, A., Krummenacker, M.,
899 Latendresse, M., Muñiz-Rascado, L., Ong, Q., Paley, S., Peralta-Gil, M.,
900 Subhraveti, P., Velázquez-Ramírez, D.A., Weaver, D., Collado-Vides, J.,
901 Paulsen, I., Karp, P.D., 2017. The EcoCyc database: Reflecting new knowledge
902 about Escherichia coli K-12. Nucleic Acids Res. 45, D543–D550.
903 https://doi.org/10.1093/nar/gkw1003
904 Khandelwal, R.A., Olivier, B.G., Röling, W.F.M., Teusink, B., Bruggeman, F.J., 2013.

905 Community Flux Balance Analysis for Microbial Consortia at Balanced Growth.
906 PLoS One. https://doi.org/10.1371/journal.pone.0064567
907 Kitano, H., 2007. Towards a theory of biological robustness. Mol. Syst. Biol.
908 https://doi.org/10.1038/msb4100179
909 Koch, S., Kohrs, F., Lahmann, P., Bissinger, T., Wendschuh, S., Benndorf, D., Reichl,
910 U., Klamt, S., 2019. Redcom: A strategy for reduced metabolic modeling of
911 complex microbial communities and its application for analyzing experimental
912 datasets from anaerobic digestion. PLoS Comput. Biol. 15.
913 https://doi.org/10.1371/journal.pcbi.1006759
914 Langmead, B., Salzberg, S.L., 2012. Fast gapped-read alignment with Bowtie 2. Nat.
915 Methods 9, 357–359. https://doi.org/10.1038/nmeth.1923
916 Lebuhn, M., Weiß, S., Munk, B., Guebitz, G.M., 2015. Microbiology and molecular
917 biology tools for biogas process analysis, diagnosis and control. Adv. Biochem.
918 Eng. Biotechnol. 151. https://doi.org/10.1007/978-3-319-21993-6_1
919 Lewis, N.E., Hixson, K.K., Conrad, T.M., Lerman, J.A., Charusanti, P., Polpitiya, A.D.,
920 Adkins, J.N., Schramm, G., Purvine, S.O., Lopez-Ferrer, D., Weitz, K.K., Eils, R.,
921 König, R., Smith, R.D., Palsson, B., 2010. Omic data from evolved E. coli are
922 consistent with computed optimal growth from genome-scale models. Mol. Syst.
923 Biol. 6. https://doi.org/10.1038/msb.2010.47
924 Liao, J.C., Mi, L., Pontrelli, S., Luo, S., 2016. Fuelling the future: Microbial engineering
925 for the production of sustainable biofuels. Nat. Rev. Microbiol.
926 https://doi.org/10.1038/nrmicro.2016.32
927 Liebetrau, J., Sträuber, H., Kretzschmar, J., Denysenko, V., Nelles, M., 2019.
928 Anaerobic digestion, in: Advances in Biochemical Engineering/Biotechnology. pp.
929 281–299. https://doi.org/10.1007/10_2016_67
930 Lieven, C., Beber, M.E., Olivier, B.G., Bergmann, F.T., Ataman, M., Babaei, P., Bartell,
931 J.A., Blank, L.M., Chauhan, S., Correia, K., Diener, C., Dräger, A., Ebert, B.E.,
932 Edirisinghe, J.N., Faria, J.P., Feist, A.M., Fengos, G., Fleming, R.M.T., García-
933 Jiménez, B., Hatzimanikatis, V., van Helvoirt, W., Henry, C.S., Hermjakob, H.,

Herrgård, M.J., Kaafarani, A., Kim, H.U., King, Z., Klamt, S., Klipp, E., Koehorst, J.J., König, M., Lakshmanan, M., Lee, D.Y., Lee, S.Y., Lee, S., Lewis, N.E., Liu, F., Ma, H., Machado, D., Mahadevan, R., Maia, P., Mardinoglu, A., Medlock, G.L., Monk, J.M., Nielsen, J., Nielsen, L.K., Nogales, J., Nookaew, I., Palsson, B.O., Papin, J.A., Patil, K.R., Poolman, M., Price, N.D., Resendis-Antonio, O., Richelle, A., Rocha, I., Sánchez, B.J., Schaap, P.J., Malik Sheriff, R.S., Shoaie, S., Sonnenschein, N., Teusink, B., Vilaça, P., Vik, J.O., Wodke, J.A.H., Xavier, J.C., Yuan, Q., Zakhartsev, M., Zhang, C., 2020. MEMOTE for standardized genome-scale metabolic model testing. Nat. Biotechnol. 38, 272–276. https://doi.org/10.1038/s41587-020-0446-y

Machado, D., Andrejev, S., Tramontano, M., Patil, K.R., 2018. Fast automated reconstruction of genome-scale metabolic models for microbial species and communities. Nucleic Acids Res. 46, 7542–7553. https://doi.org/10.1093/nar/gky537

Machado, D., Maistrenko, O.M., Andrejev, S., Kim, Y., Bork, P., Patil, Kaustubh R., Patil, Kiran R., 2020. Polarization of microbial communities between competitive and cooperative metabolism. bioRxiv 2020.01.28.922583. https://doi.org/10.1101/2020.01.28.922583

Magnúsdóttir, S., Heinken, A., Kutt, L., Ravcheev, D.A., Bauer, E., Noronha, A., Greenhalgh, K., Jäger, C., Baginska, J., Wilmes, P., Fleming, R.M.T., Thiele, I., 2017. Generation of genome-scale metabolic reconstructions for 773 members of the human gut microbiota. Nat. Biotechnol. 35, 81–89. https://doi.org/10.1038/nbt.3703

Mas, A., Jamshidi, S., Lagadeuc, Y., Eveillard, D., Vandenkoornhuyse, P., 2016. Beyond the Black Queen Hypothesis. ISME J. https://doi.org/10.1038/ismej.2016.22

Maus, I., Cibis, K.G., Bremges, A., Stolze, Y., Wibberg, D., Tomazetto, G., Blom, J., Sczyrba, A., König, H., Pühler, A., Schlüter, A., 2016. Genomic characterization of Defluviitoga tunisiensis L3, a key hydrolytic bacterium in a thermophilic biogas

963 plant and its abundance as determined by metagenome fragment recruitment. J.
964 Biotechnol. 232, 50–60. https://doi.org/10.1016/j.jbiotec.2016.05.001
965 Mendes-Soares, H., Mundy, M., Soares, L.M., Chia, N., 2016. MMinte: An application
966 for predicting metabolic interactions among the microbial species in a community.
967 BMC Bioinformatics 17. https://doi.org/10.1186/s12859-016-1230-3
968 Moat, A.G., Foster, J.W., Spector, M.P., 2002. Microbial Physiology, Microbial
969 Physiology. https://doi.org/10.1002/0471223867
970 Molina, F., Ruiz-Filippi, G., Garcia, C., Lema, J.M., Roca, E., 2009. Pilot-scale
971 validation of a new sensor for on-line analysis of volatile fatty acids and alkalinity
972 in anaerobic wastewater treatment plants. Environ. Eng. Sci. 26, 641–649.
973 https://doi.org/10.1089/ees.2007.0308
974 Mosbæk, F., Kjeldal, H., Mulat, D.G., Albertsen, M., Ward, A.J., Feilberg, A., Nielsen,
975 J.L., 2016. Identification of syntrophic acetate-oxidizing bacteria in anaerobic
976 digesters by combined protein-based stable isotope probing and metagenomics.
977 ISME J. 10, 2405–2418. https://doi.org/10.1038/ismej.2016.39
978 Muller, E.E.L., Faust, K., Widder, S., Herold, M., Martínez Arbas, S., Wilmes, P., 2018.
979 Using metabolic networks to resolve ecological properties of microbiomes. Curr.
980 Opin. Syst. Biol. https://doi.org/10.1016/j.coisb.2017.12.004
981 Nayfach, S., Shi, Z.J., Seshadri, R., Pollard, K.S., Kyrpides, N.C., 2019. New insights
982 from uncultivated genomes of the global human gut microbiome. Nature 568,
983 505–510. https://doi.org/10.1038/s41586-019-1058-x
984 Niehaus, L., Boland, I., Liu, M., Chen, K., Fu, D., Henckel, C., Chaung, K., Miranda,
985 S.E., Dyckman, S., Crum, M., Dedrick, S., Shou, W., Momeni, B., 2019. Microbial
986 coexistence through chemical-mediated interactions. Nat. Commun. 10.
987 https://doi.org/10.1038/s41467-019-10062-x
988 Noronha, A., Modamio, J., Jarosz, Y., Guerard, E., Sompairac, N., Preciat, G.,
989 Daníelsdóttir, A.D., Krecke, M., Merten, D., Haraldsdóttir, H.S., Heinken, A.,
990 Heirendt, L., Magnúsdóttir, S., Ravcheev, D.A., Sahoo, S., Gawron, P., Friscioni,
991 L., Garcia, B., Prendergast, M., Puente, A., Rodrigues, M., Roy, A., Rouquaya,

M., Wiltgen, L., Žagare, A., John, E., Krueger, M., Kuperstein, I., Zinovyev, A., Schneider, R., Fleming, R.M.T., Thiele, I., 2019. The Virtual Metabolic Human database: Integrating human and gut microbiome metabolism with nutrition and disease. Nucleic Acids Res. 47, D614–D624. https://doi.org/10.1093/nar/gky992

Nugent, P., Giannopoulou, E.G., Burd, S.D., Elemento, O., Giannopoulou, E.G., Forrest, K., Pham, T., Ma, S., Space, B., Wojtas, L., Eddaoudi, M., Zaworotko, M.J., 2013. Porous materials with optimal adsorption thermodynamics and kinetics for co2 separation. Nature 495, 80–84. https://doi.org/10.1038/nature11893

Oki, E., 2012. GLPK (GNU Linear Programming Kit), in: Linear Programming and Algorithms for Communication Networks. pp. 25–29. https://doi.org/10.1201/b12733-4

Parks, D.H., Rinke, C., Chuvochina, M., Chaumeil, P.A., Woodcroft, B.J., Evans, P.N., Hugenholtz, P., Tyson, G.W., 2017. Recovery of nearly 8,000 metagenome-assembled genomes substantially expands the tree of life. Nat. Microbiol. 2, 1533–1542. https://doi.org/10.1038/s41564-017-0012-7

Raspor, P., Goranovič, D., 2008. Biotechnological applications of acetic acid bacteria. Crit. Rev. Biotechnol. https://doi.org/10.1080/07388550802046749

Shlomi, T., Eisenberg, Y., Sharan, R., Ruppin, E., 2007. A genome-scale computational study of the interplay between transcriptional regulation and metabolism. Mol. Syst. Biol. 3. https://doi.org/10.1038/msb4100141

Sorokin, Di.Y., Makarova, K.S., Abbas, B., Ferrer, M., Golyshin, P.N., Galinski, E.A., Ciordia, S., Mena, M.C., Merkel, A.Y., Wolf, Y.I., Van Loosdrecht, M.C.M., Koonin, E. V., 2017. Discovery of extremely halophilic, methyl-reducing euryarchaea provides insights into the evolutionary origin of methanogenesis. Nat. Microbiol. 2. https://doi.org/10.1038/nmicrobiol.2017.81

Stams, A.J.M., 1994. Metabolic interactions between anaerobic bacteria in methanogenic environments. Antonie Van Leeuwenhoek 66, 271–294. https://doi.org/10.1007/BF00871644

1021 Stams, A.J.M., Plugge, C.M., 2009. Electron transfer in syntrophic communities of
1022 anaerobic bacteria and archaea. Nat. Rev. Microbiol.
1023 https://doi.org/10.1038/nrmicro2166
1024 Stolyar, S., Van Dien, S., Hillesland, K.L., Pinel, N., Lie, T.J., Leigh, J.A., Stahl, D.A.,
1025 2007. Metabolic modeling of a mutualistic microbial community. Mol. Syst. Biol. 3,
1026 1–14. https://doi.org/10.1038/msb4100131
1027 Stryer, L., 1995. Stryer Biochemistry, Biochemistry textbook.
1028 Thommes, M., Wang, T., Zhao, Q., Paschalidis, I.C., Segrè, D., 2019. Designing
1029 Metabolic Division of Labor in Microbial Communities. mSystems 4.
1030 https://doi.org/10.1128/msystems.00263-18
1031 Treu, L., Campanaro, S., Kougias, P.G., Sartori, C., Bassani, I., Angelidaki, I., 2018.
1032 Hydrogen-fueled microbial pathways in biogas upgrading systems revealed by
1033 genome-centric metagenomics. Front. Microbiol. 9.
1034 https://doi.org/10.3389/fmicb.2018.01079
1035 Treu, L., Tsapekos, P., Peprah, M., Campanaro, S., Giacomini, A., Corich, V.,
1036 Kougias, P.G., Angelidaki, I., 2019. Microbial profiling during anaerobic digestion
1037 of cheese whey in reactors operated at different conditions. Bioresour. Technol.
1038 275, 375–385. https://doi.org/10.1016/j.biortech.2018.12.084
1039 Weinrich, S., Koch, S., Bonk, F., Popp, D., Benndorf, D., Klamt, S., Centler, F., 2019.
1040 Augmenting biogas process modeling by resolving intracellular metabolic activity.
1041 Front. Microbiol. 10. https://doi.org/10.3389/fmicb.2019.01095
1042 Westerholm, M., Dolfing, J., Schnürer, A., 2019. Growth Characteristics and
1043 Thermodynamics of Syntrophic Acetate Oxidizers. Environ. Sci. Technol. 53,
1044 5512–5520. https://doi.org/10.1021/acs.est.9b00288
1045 Yentekakis, I. V., Goula, G., 2017. Biogas management: Advanced utilization for
1046 production of renewable energy and added-value chemicals. Front. Environ. Sci.
1047 https://doi.org/10.3389/fenvs.2017.00007
1048 Zacher, B., Lidschreiber, M., Cramer, P., Gagneur, J., Tresch, A., 2014. Annotation of
1049 genomics data using bidirectional hidden Markov models unveils variations in Pol

II transcription cycle. Mol. Syst. Biol. 10, 768. https://doi.org/10.15252/msb.20145654

Zhu, X., Campanaro, S., Treu, L., Kougias, P.G., Angelidaki, I., 2019. Novel ecological insights and functional roles during anaerobic digestion of saccharides unveiled by genome-centric metagenomics. Water Res. 151, 271–279. https://doi.org/10.1016/j.watres.2018.12.041

Zhu, X., Campanaro, S., Treu, L., Seshadri, R., Ivanova, N., Kougias, P.G., Kyrpides, N., Angelidaki, I., 2020. Metabolic dependencies govern microbial syntrophies during methanogenesis in an anaerobic digestion ecosystem. Microbiome 8. https://doi.org/10.1186/s40168-019-0780-9

Zomorrodi, A.R., Maranas, C.D., 2012. OptCom: A multi-level optimization framework for the metabolic modeling and analysis of microbial communities. PLoS Comput. Biol. 8. https://doi.org/10.1371/journal.pcbi.1002363